A STATISTICAL HOT SPOT REACTIVE FLOW MODEL FOR SHOCK INITIATION AND DETONATION OF SOLID HIGH EXPLOSIVES *

Albert L. Nichols III and Craig M. Tarver
Lawrence Livermore National Laboratory
Livermore, CA 94551

A statistical hot spot reactive flow model for shock initiation and detonation of solid high explosives developed in the ALE3D hydrodynamic computer code is presented. This model is intended to evolve into a physically correct description of the physical and chemical mechanisms that control the onset of shock initiation via hotspot formation, the growth (or failure to grow) of these hotspots into the surrounding explosive particles, the rapid transition to detonation, and self-sustaining detonation. Mesoscale modeling of the shock compression and temperature dependent chemical decomposition of individual explosive particles are currently yielding accurate predictions of hot spot formation and the subsequent growth (or failure) of these hotspot reactions in the surrounding grains. For two- and three-dimensional simulations of larger scale explosive charges, a statistical hotspot model that averages over thousands of individual hotspot dimensions and temperatures and then allows exothermic chemical reactions to grow (or fail to grow) due to thermal conduction is required. This paper outlines a first approach to constructing a probabilistic hot spot formulation based on the number density of potential hotspot sites. These hotspots can then either ignite or die out if they do not exceed certain ignition criteria, which are based on physical properties of the explosive particles. The growing hot spots spread at burn velocities given by experimentally determined deflagration velocity versus pressure relationships. The mathematics and assumptions involved in formulating the model and examples of shock initiation and desensitization modeling are given.

INTRODUCTION

Phenomenological reactive flow models for the shock initiation and detonation of solid high explosives, such as the Ignition and Growth model[1,2] and the Johnson-Tang-Forest (JTF) model[3] have been very successful in reproducing most of the main features of these reactive flows. The reaction rate expressions in these models depend upon the average compressions and pressures attained in the reacting explosive mixture rather than the local "hot spot" temperatures, which are known to control the reaction rates in the preferentially heated regions of the explosive charge. Thus there are some situations, such as shock desensitization[4], that are not easily treated by these phenomenological models. Mesoscale modeling of the shock compression[5] and temperature dependent chemical decomposition[6] of individual explosive particles are currently yielding accurate predictions of hot spot formation mechanisms and the subsequent growth (or failure) of these hot spot reactions in the surrounding grains. For two- and three-dimensional simulations of realistic size explosive charges, a statistical hot spot model that averages over thousands of individual hot spot dimensions and temperatures and then allows the chemical reactions to grow (or fail to grow) due to thermal conduction is required. Some simple statistical hot spot models were developed several years ago in one-dimensional hydrodynamic codes[7,8], but practical hot spot models in multidimensional codes are just beginning to appear.

The chemical kinetic decomposition models for HMX and TATB used in this statistical model have been previously used to determine the critical hot spot temperatures and dimensions that will react and begin to grow[9]. The growth rates of these hot spots due only to thermal conduction were also determined[10], and were shown to be too slow to account for measured shock initiation times and run distances to detonation. Therefore physical mechanisms, such as crack nucleation and growth, must be causing greatly increased reactive surface area as the pressure and temperature increase during shock initiation and the transition to detonation.

In this paper, the formulation of a statistical hot spot creation model in the ALE3D hydrodynamic code is presented. During shock compression, a distribution of "hotspot" sizes and temperatures based on the initial pore size distribution, explosive

particle size distribution, and the density of the explosive charge is created. These hot spots then grow to consume neighboring explosive particles or fail to grow as thermal conduction lowers their temperature before exothermic chemical reaction can be completed. The growth rate of the surviving hot spots is then modeled by a statistical hotspot growth model normalized to experimental high-pressure deflagration rate data. The coalescence of these expanding hot spots as the temperature and pressure rapidly rise everywhere in the decomposing explosive charge is also discussed. The extremely rapid transition to detonation observed experimentally is shown to be similar to a constant volume explosion from a critical compression state of the unreacted explosive to a state on the reaction product Hugoniot close to the Chapman-Jouguet (C-J) state. Examples of calculated shock initiation and detonation wave propagation for an HMX-based explosive are presented. Examples of shock initiation effects, such as desensitization and changes in sensitivity due to initial temperature and particle size distribution variations, that are difficult or impossible to compute with pressure and compression dependent reactive flow models are also presented.

STATISTICAL HOTSPOT MODEL

PROBABILISTIC HOTSPOT FORMULATION

The first phase in constructing the statistical hot spot model is the consideration of the distribution of those hot spots. First, consider the probability P_r that single hotspot of radius R will have reacted at a given location in a volume V in the explosive. This probability is given by:

$$P_r = \frac{4\pi R^3}{3V} \tag{1}$$

If there are N_R of these hotspots randomly distributed in space, then the probability that a given location has *not* reacted P_{nr} is simply the product of the independent probabilities. Assuming that the hot spots are independently located, P_{nr} is defined as:

$$P_{nr} = \left(1 - \frac{4\pi R^3}{3V}\right)^{N_R} \tag{2}$$

Taking the limit where the volume becomes large but the hotspot density remains fixed, Eq. (2) becomes:

$$P_{nr}(R) = \exp\left(-\frac{4\pi R^3}{3}\rho(R)\right) \tag{3}$$

Finally, the combined probability of a region not having been reacted $P_{nr}(R)$ is simply the product of the probabilities associated with each hotspot radius. Therefore the final expression for P_{nr} is:

$$P_{nr} = \exp\left(-\frac{4\pi}{3}\int_0^\infty R^3\rho(R)dR\right) \tag{4}$$

The probability of not yet reacting is simply the mass fraction of the reactant in a reactive flow formulation. The probabilistic formulation makes it easier to consider a variety of different possibilities. For example, a similar line of reasoning can be used for two-dimensional hotspots (hotlines) and one-dimensional hotspots (hotplanes). The latter would be useful for the modeling of shear banding as an ignition source, for example. If all of such ignition mechanisms could be defined, all that would be required for a complete hot spot model is to multiply their probability functions together.

HOTSPOT DENSITY MODEL

The process derived in the previous section defines a mechanism for connecting the probability that some quantity of explosive has been reacted to the density distribution of hotspots. We define the probability density of the hotspots as:

$$\rho(R,t) = \rho_A(R,t) + \rho_D(R,t) \tag{5}$$

$$\rho_A(R,t) = \int_{-\infty}^{t} d\alpha \int_{t}^{\infty} d\omega\, \rho_s(\alpha,\omega)\delta\left(R-\varepsilon-\int_{\alpha}^{t} d\tau v(\tau)\right) \quad (6)$$

$$\rho_D(R,t) = \int_{-\infty}^{t} d\alpha \int_{-\infty}^{t} d\omega\, \rho_s(\alpha,\omega)\delta\left(R-\varepsilon-\int_{\alpha}^{\omega} d\tau v(\tau)\right) \quad (7)$$

where $\rho_s(\alpha,\omega)$ is the number density of hotspots that ignited at time α, and died at time ω. The dirac-delta functions are used to define the size of the hotspot with the assumption that the initial hotspot size is ε, and that it then burns at a burn rate v out from that initial spot. The first term $\rho_A(R,t)$ represents the population of hotspots of size R that are still growing (active) at time t. The second term $\rho_D(R,t)$ represents the population of hotspots of size R that have stopped growing (died) by time t. It is important to remember that even though a hotspot may stop burning, the material that has burned within that hotspot must still be counted as reacted.

Let us now define the following projections of the density function:

$$\begin{aligned} h(t) &= \frac{4\pi}{3}\int_0^\infty dR\, R^3 \rho(R,t) \\ \bar{g}(t) &= \pi \int_0^\infty dR\, R^2 \rho_A(R,t) \\ \bar{f}(t) &= 2\int_0^\infty dR\, R \rho_A(R,t) \\ \bar{\rho}_A(t) &= \int_{-\infty}^{t} d\alpha \int_t^\infty d\omega\, \rho_s(\alpha,\omega) \\ \rho_B(t) &= \int_t^\infty d\omega\, \rho_s(t,\omega) \end{aligned} \quad (8)$$

The h term is just the negative of the log of the probability defined in Eq. (4). The g and f terms are the two- and one-dimensional active projections of the density function, respectively. The number of hotspots that are active at time t is $\bar{\rho}_A(t)$, and $\rho_B(t)$ is the number of hotspots created at time t. In the current model, it is assumed that all hotspots active at time t have the same rate of death $\mu(t)$, that is:

$$\rho_s(\alpha,t) = \mu(t)\int_t^\infty \rho_s(\alpha,\omega) \quad (9)$$

With these projections, it is possible to construct a set of differential equations to couple the high order unreacted mass fraction with the much simpler active hotspot density.

$$\begin{aligned} \frac{\partial h}{\partial t} &= 4v(t)\bar{g}(t) + 4\pi\varepsilon^3\rho_B(t)/3 \\ \frac{\partial \bar{g}}{\partial t} &= \pi v(t)\bar{f}(t) + 4\pi\varepsilon^2\rho_B(t) - \mu(t)\bar{g}(t) \\ \frac{\partial \bar{f}}{\partial t} &= 2v(t)\bar{\rho}_A(t) + 2\varepsilon\rho_B(t) - \mu(t)\bar{f}(t) \\ \frac{\partial \bar{\rho}_A}{\partial t} &= \rho_B(t) - \mu(t)\bar{\rho}_A(t) \end{aligned} \quad (10)$$

IGNITION MODEL

In order to complete the set of equations defined in the previous section, we must define the rate at which hotspots are created. In order to model the explosive process, it is necessary to choose an ignition model that can encompass a variety of phenomena associated with high explosives. We begin by defining the initial density of potential hotspots ρ_P^0. These potential hotspots can be anything from defects in the crystal lattice to voids in the region between the explosive grains. For the current model, we only limit ourselves in that the potential hotspot must transform into a roughly spherical hotspot. Most postulated hotspot formation mechanisms involving void collapse predict that the spherical hotspots form upon full collapse[11]. Other potential hotspot formation mechanisms, such as shear banding, would transform into roughly planar hotspots and thus are not considered in this

treatment. The shock process compresses these potential hotspots. If they are compressed to a sufficiently high temperature, they will start to react (a hotspot). If the process is too weak, then the potential hotspot will be destroyed without creating a hotspot. Without such a process, any sufficient compression of the explosive would lead to reaction, even that from an isostatic press. However, since explosives do have strength, there must be sufficient force to overcome that internal void strength before any changes to the potential hotspot density can occur. The following phenomenological ignition model captures these features.

$$\mathrm{K} = \left(\frac{AP^*\left(P - P_0\right)}{P^* + P - P_0} \right) H\left(P - P_0\right) \tag{11}$$

$$\begin{aligned} \dot{\rho}_P &= -\rho_P \mathrm{K} \\ \rho_B &= \rho_P \left(\mathrm{K} - D\right) H\left(\mathrm{K} - D\right) \end{aligned} \tag{12}$$

Here K is the rate of potential hotspot transformation, and *D* is the constant death rate for potential hotspots. P_0 is the ignition rate threshold pressure that represents the internal resistance to void collapse. To prevent unrealistically large collapse rates during numerical pressure spikes, P^* is defined as the saturation pressure. *H* is the heavy side step function, which is zero for all arguments less than zero and one for everything else. We originally envisioned a compression rate dependent ignition rate, but such a rate can be extremely mesh-size dependent. More complex ignition models can be formulated as this model evolves.

PHYSICAL INTERPRETATION OF HOTSPOT MODEL PARAMETERS

We have defined a total of 8 parameters, not counting those associated with the equation of state, for this model. They are: P_0, P^*, A, μ, v, D, ρ_P^0, and ε. P_0 is clearly related to the yield strength of the explosive, and so we will use the yield strength in our model. The burn velocity *v* can be experimentally determined by any of the standard burn rate measurement techniques, such as strand-burner and diamond anvil experiments. The value of D should be chosen to match explosive shock recovery experiments, so that the value of D is set equal to the value of R for the shock pressure that just begins to ignite the explosive.

A heuristic argument can be used to determine ρ_P^0, and ε. If one assumes that the initial hotspot volume will equal the initial void volume and that enough hotspots need to be created so that when they burn they will consume the entire explosive in the reaction zone time τ and initial void density ρ_v:

$$\begin{aligned} \rho_v &\approx 4\pi\varepsilon^3 \rho_P^0 / 3 \\ 1 &\approx 4\pi\left(\varepsilon + v\tau\right)^3 \rho_P^0 / 3 \end{aligned} \tag{13}$$

Another heuristic argument can be applied to the ignition pre-factor A and P^*. It is reasonable to assume that the rate of collapse of the void regions is proportional to the product of the void radius and the particle velocity *u* in the shock wave. For relatively low pressures, we can Taylor expand the volume change using the adiabatic compressibility, and get:

$$\begin{aligned} R &\approx \frac{u}{2\varepsilon} \approx \frac{1}{2\varepsilon}\sqrt{\frac{\left(P - P_0\right)\left(\rho - \rho_0\right)}{\rho\rho_0}} \\ &\approx \left(P - P_0\right) / \left(2\varepsilon\rho_0 c\right) \end{aligned} \tag{14}$$

where ρ_0 is the initial density, and *c* is the reference sound speed. Comparing to the ignition definition in the limit of small $(P\text{-}P_0)$, we find

$$A \approx \frac{1}{\left(2\varepsilon\rho_0 c\right)} \tag{15}$$

Although it might be tempting to use an ignition form defined by the particle velocity, the complexities associated with making it work under the variety initial conditions would be daunting. For example, changes in temperature would necessitate a change in the reference density within the root sign. Without such a change, hot systems could never ignite. We can handle the natural curvature that comes out of this formulation by an appropriate choice of P^*.

TABLE 1. PRESSURE VERSUS BURN RATE

PRESSURE (GPa)	BURN RATE (cm/μs)
1.0×10^{-4}	1.016×10^{-7}
1.151×10^{-2}	9.068×10^{-7}
3.842×10^{-2}	1.763×10^{-6}
5.957×10^{-2}	3.599×10^{-6}
8.077×10^{-2}	6.988×10^{-4}
1.164×10^{-1}	1.016×10^{-3}
1.0	4.441×10^{-3}

EXAMPLE PROBLEMS

SHOCK INITIATION

The phenomenological reactive flow model Ignition and Growth[1] has been normalized to a great deal of shock initiation data. However, for different initial temperatures and particle size distributions, it has to be reparameterized. The Statistical Hot Spot model has the necessary features to calculate such initial condition differences. The first example problem is to drive a 2 cm wide by 3 cm long by 0.1 cm deep block of explosive into a stone wall to check the two-dimensional shock initiation characteristics of the Statistical Hot Spot model. As previously mentioned, an unreacted equation of state is needed to describe the states attained during shock compression. The Jones-Wilkins-Lee (JWL) equation of state is used with typical parameters for an HMX-based plastic bonded explosive.

$$P = A\left(1-\frac{\omega}{R_1 V}\right)e^{-R_1 V} - B\left(1-\frac{\omega}{R_{12} V}\right)e^{-R_{21} V} + \frac{\omega E}{V} \qquad (16)$$

where P is pressure, V is relative volume, E is the internal energy, ω is the Gruneisen coefficient, and A, B, R_1, and R_2 are constants. For a typical HMX-based plastic bonded explosive, the initial density is 1.85 g/cm^3, R_1 = 14.1, R_2 = 1.41, ω = 0.8938, A = 9522 Mbar, and B = 0.05944 Mbar. This JWL equation fits the measured unreacted Hugoniot data at low shock pressures and the von Neumann spike data at high pressures[12]. The reaction products are described by LEOS tables fit to product Hugoniot states and isentropes calculated by the CHEETAH chemical equilibrium code[13]. Mixtures of unreacted explosive and reaction products are assumed to be in pressure equilibrium.

As discussed in the previous section, the ignition and growth of reaction model has eight parameters: P_0, P^*, A, μ, v, D, ρ_P^0, and ε. P_0 is the ignition rate threshold pressure, which is related to the effective yield strength at high strain rates and is set equal to 0.1 GPa for these calculations. P* is the saturation pressure below which all hot spots are formed and is set equal to 10 GPa. The ignition prefactor A is defined by Eq. (15) and, for HMX, is approximately 2000 cm-μs/g. The hot spot death rate μ is initially set equal to 5 μs^{-1}. The constant death rate parameter for potential hot spot D is set equal to 11.3. The initial number of potential hot spot sites ρ_P is assumed to be 1.4×10^{10} cm^{-3}. The initial hot spot diameter ε is assumed to be 1.5×10^{-4} cm or 1.5 μm. The reaction growth rate v is assumed to be a function of pressure as measured experimentally in strand burners[14]. This pressure versus burn rate function is shown in Table 1.

Using these input values, the explosive was driven into a stonewall at various velocities to study the buildup of the shock wave produced in the explosive to a detonation. In agreement with numerous experiments and previous models, the buildup toward detonation occurred well behind the shock front, the transition to detonation was rapid, and the resulting detonation wave traveled at the

TABLE 2. INITIAL CONDITIONS AND TIMES TO COMPLETE REACTION

VELOCITY (mm/μs)	REACTION TIMES (μs)
0.18	2.51
0.30	2.27
0.60	1.70
1.2	1.51
2.4	0.29

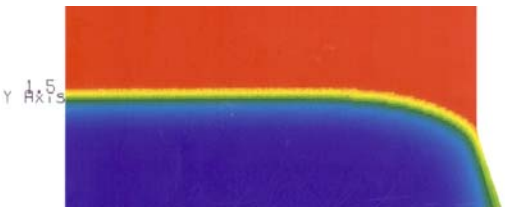

FIGURE 1. FRACTION REACTED FOR HMX (RED – 0%; BLUE – 100%) AT 2.33 μs FOR AN INITIAL VELOCITY OF 0.3 mm/μs

correct velocity, 8.8 mm/μs. Table 2 lists the initial velocities and the calculated times to complete reaction. These reaction times are reasonable for HMX-based plastic bonded explosives. Figure 1 shows the fraction reacted contours for HMX decomposition at 2.33 μs for the 0.3 mm/μs initial velocity case.

The effects of changing various hot spot parameters were investigated using an initial particle velocity of 0.18 mm/μs or an initial shock pressure of approximately 1 GPa. Reducing the hot spot death rate parameter μ from 5 to 1 reduced the time to complete reaction from 2.51 μs to 1.76 μs, and increasing μ to 10 caused the fraction reaction to remain below 0.45. Lowering the constant death rate parameter D to 1.13 from 11.3 led to complete reaction in 2.3 μs instead of 2.51 μs, and raising D to 22.6 forced no reaction to occur in 9.3 μs.

One important effect on shock initiation is the initial particle size effect, which controls both the initial number of hot spot sites and the size distribution of these sites. Every solid explosive exhibits a maximum shock sensitivity at a certain particle size. If the particles are large, there are larger sites but they are easily compressed resulting in relatively temperatures.[6] If the particles are small, there are more small sites compressed to high

TABLE 3. EFFECT OF HOT SPOT DENSITY

Sites(cm^{-3})	Fraction Reacted	Time (μs)
1.4×10^{9}	0.0523	4.09
1.4×10^{10}	0.954	1.92
1.4×10^{11}	0.976	0.114

TABLE 4. EFFECT OF HOT SPOT SIZE

Diameter (cm)	Fraction Reacted	Time (μs)
3.0×10^{-4}	0.979	0.29
1.5×10^{-4}	0.954	1.92
9.0×10^{-5}	0.1792	5.86
6.0×10^{-5}	0.0322	10.52

temperatures, but many of these hot spots cool by conduction before they can react and grow.[6] Table 3 shows the effects of changing the initial number of potential hot spots ρ_P by an order of magnitude in each direction. Large particle size formulations contain fewer sites and thus are less shock sensitive.

Table 4 shows the effects of initial hot spot diameter ε on the reaction times. Figure 2 shows the fraction reacted for the 0.6-micron diameter case at a time of 10.52 μs when the shock wave has traveled through the 3 cm long charge. The 0.6 and 0.9 micron results ignite approximately the correct amount of fraction reacted for shock initiation studies, and are reasonable hot spot sizes for real solid explosive formulations. Since the reaction rate falls rapidly with decreasing hot spot size and number of hot spot sites, the Statistical Hot Spot model is predicting the well-known particle size effects on shock initiation of solid explosives.

The pressure versus reaction rate function for hot spot growth shown in Table 1 is similar to deflagration rates observed in strand burners at pressures below 1 GPa. For the higher pressures

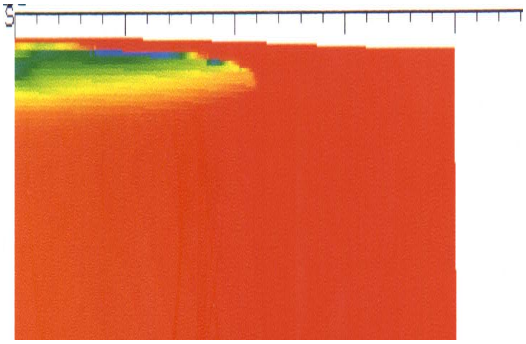

FIGURE 2. HMX FRACTION REACTED AT 10.52 μs FOR 0.6 μm DIAMETER HOT SPOTS IMPACTED AT AN INITIAL VELOCITY OF 0.18 mm/μs

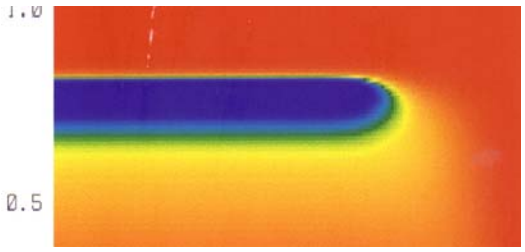

FIGURE 3. HMX FRACTED REACTED AT 2.97 μs FOR 1.5 μm DIAMETER HOT SPOTS IMPACTED AT 0.18 mm/μs

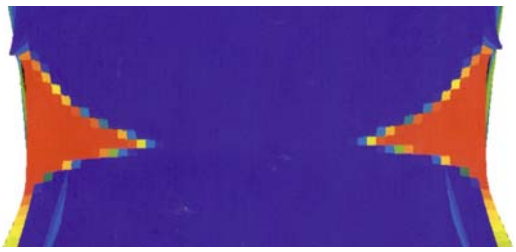

FIGURE 4. COLLISION OF TWO CURVED HMX DETONATION WAVES

reached during shock initiation and detonation, the growth rate function was fit to recent diamond anvil cell (DAC) burn rate data on pure HMX[15] by Reaugh.[6] These rates are shown in Table 5 and are much faster than those in Table 1. With this faster burn rate function, less hot spot ignition is required for realistic reaction buildup times. Table 6 shows the effects of hot spot size in conjunction with the DAC based growth rates. Figure 3 shows the fraction reacted contours at 2.97 ms for the 1.5 micron hot spot diameter case. These examples of shock initiation demonstrate some of the capabilities of the Statistical Hot Spot model. The current parameters will be fine-tuned for specific explosive formulations.

COLLIDING SHOCK & DETONATION WAVES

The other main area where phenomenological reactive flow models sometimes have problems is when multiple shock or detonation waves collide, yielding regions of very high pressure and reaction rates. To test the ability of the Statistical Hot Spot model to handle such problems, the explosive block described above was initiated on the top and bottom by imparting initial pressures to start the reaction sequence. Figure 4 shows the collision of the curved detonation waves with unreacted HMX at the edges still being consumed. Since the reaction rates at very high pressures (essentially twice the detonation pressure in this example) are limited in the Statistical Hot Spot model, the calculation times do not increase dramatically as they can using models with pressure dependent reaction rates. The ALE3D code can overcome the deformed zone problems that purely Lagrange codes often cannot under these conditions. This capability will be extremely important when the complex three-dimensional Mach stem structure of real detonation waves is simulated in three dimensions.

One of the most important and complex modeling problems in solid explosives is the phenomena of "shock desensitization" or "dead pressing." The most famous experimental example is that of Campbell and Travis[4], in which a PBX 9404 is detonated at one end and a weak shock wave from an underwater detonation impacts the same PBX 9404 charges at the other end. If this shock wave is too weak to collapse all the potential hot spot sites, then the detonation propagates through this semi-compressed material. If the shock wave is

TABLE 5. PRESSURE VERSUS DAC BURN RATES

PRESSURE (GPa)	Burn Rate (cm/μs)
1.0×10^{-4}	2.35×10^{-7}
1.0×10^{-1}	5.0×10^{-5}
3.0	7.0×10^{-4}
50	9.0×10^{-2}
200	0.9852

TABLE 6. HOT SPOT SIZE EFFECTS WITH DAC BURN RATES

Diameter(μm)	Fraction Reacted	Time(μs)
0.9	1.0	0.84
0.6	1.0	1.44
0.3	1.0	2.36
0.15	1.0	2.97

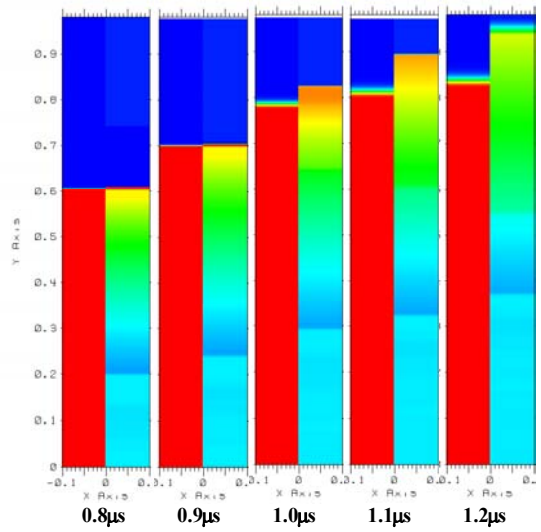

FIGURE 5. SHOCK DESENSITIZATION PRODUCED BY THE COLLISION OF A SHOCK (AT TOP) AND A DETONATION (BOTTOM) AT 0.9 μs; FRACTION REACTED (BLUE - 0%; RED - 100 %) ON LEFT AND PRESSURE ON RIGHT

strong enough to start hot spot ignition and growth, then the detonation wave continues through the partly reacted explosive. However, if the shock wave pressure is within a certain range (0.7 to 2.4 GPa for PBX 9404) which collapses all the potential hot spot sites without causing reaction growth, then the detonation wave will fail to propagate when it reaches a depth at there are only "dead" or burned out hot spots and unreacted particles. Composition B-3,[4] the TATB-based explosive LX-17[16], and other explosives have also been shown to exhibit this phenomena. Phenomenological reactive flow models can be parameterized to not allow reaction in certain compression regimes[16] or to use reaction rate limitations[17], but they can not predict the times required for the "death" of a detonation wave.

Figure 5 shows the collision of a detonation wave with a region of explosive compacted by a shock pressure of 1 GPa at 0.9 μs and the resulting failure of the detonation wave to cause further reaction at later times in the pre-compressed explosive whose hot spot sites have already died or reacted. In Fig. 5, the fraction reacted (blue – no reaction; red – 100% reaction) is shown on the left hand side of each of the five time snapshots, while pressure (dark blue represents low pressure and light blue represents detonation pressure) is shown on the right hand side. After the collision, the detonation wave continues into the pre-compressed explosive at a slightly higher velocity due to the higher density of the pre-shocked material (time = 1.0 μs in Fig. 5). At later times, the fraction reacted stops propagating into the pre-compressed explosive and the pressure decreases, indicating that the detonation wave is falling to propagate. The classic experiments of Campbell and Travis[4] showed that the failure of the detonation in the desensitized explosive required times close to those necessary for shock initiation. Further work is required to develop quantitative hot spot creation/destruction parameters for the shock desensitization of PBX 9404, Composition B-3, and LX-17. However, the current results show that the Statistical Hot Spot model is definitely capable of quantitatively modeling shock desensitization, particle size effects on shock initiation and detonation wave propagation in three dimensions.

CONCLUSIONS

In this paper, a statistical hot spot model is derived that can be applied to situations that are normally not possible to model with a more standard reactive flow treatment. Examples are shown for the effects of initial shock pressure, hot spot size, hot spot number density, and high pressure deflagration growth rates on shock initiation of an HMX-based plastic bonded explosive. Examples for the collision of two detonation waves and of a weak shock with a detonation resulting in shock desensitization demonstrate the versatility of the model. More research is necessary to study the combined effects of the various parameters and to make each part of the model as physically realistic as possible.

ACKNOWLEDGMENTS

The authors would like to thank Estella M. McGuire for doing most of the ALE3D calculations. Helpful discussions with Jack Reaugh and Melvin Baer are gratefully acknowledged.

*This work performed under the auspices of the U.S. Department of Energy by the University of California, Lawrence Livermore National Laboratory under Contract W-7405-Eng-48.

REFERENCES

1. Tarver, C. M., Hallquist, J. O., and Erickson, L. M., "Modeling Short Shock Pulse Duration Shock Initiation of Solid Explosives," Eighth Symposium (International) on Detonation, Naval Surface Weapons Center NSWC 86-194, Albuquerque, NM, 1985, p. 951.

2. Tarver, C. M., Kury, J. W., and Breithaupt, R. D., "Detonation Waves in Triaminotrinitrobenzene," J. Appl. Phys. **82**, 3771(1997).

3. Johnson, J. N., Tang, P. K., and Forest, C. A., "Shock-Wave Initiation of Heterogeneous Reactive Solids," J. Appl. Phys. **57**, 4323 (1985).

4. Campbell, A. W. and Travis, J. R., "The Shock Desensitization of PBX-9404 and Composition B-3," Eighth Symposium (International) on Detonation, Naval Surface Weapons Center NSWC 86-194, Albuquerque, NM, 1985, p. 1057.

5. Baer, M. R., Kipp, M. E., and van Swol, F., "Micromechanical Modeling of Heterogeneous Energetic Materials," Eleventh International Detonation Symposium, Office of Naval Research ONR 33300-5, Snowmass, CO, 1998, p. 788.

6. Reaugh, J. E., Lawrence Livermore National Laboratory, Private Communication, 2002.

7. Cochran, S. G. and Tarver, C. M., "Modeling Particle Size and Initial Temperature Effects on Shock Initiation of TATB-Based Explosives," Shock Waves in Condensed Matter-1983, J. R. Asay, R. A. Graham and G. K. Straub, eds., Elsevier Publishers B. V., 1984, p. 593.

8. Partom, Y., "A Void Collapse Model for Shock Initiation," Seventh Symposium (International) on Detonation, Naval Surface Weapons Center NSWC MP 82-334, Annapolis, MD, 1981, p. 506.

9. Tarver, C. M., Chidester, S. K., and Nichols, A. L. III, "Critical Conditions for Impact- and Shock Induced Hot Spots in Solid Explosives," J. Phys. Chem. **100**, 5794 (1996).

10. Tarver, C. M. and Nichols, A. L. III, "Hot Spot Growth in a Thermal-Chemical-Mechanical Reactive Flow Model for Shock Initiation of Solid Explosives," Eleventh International Detonation Symposium, Office of Naval Research ONR 33300-5, Snowmass, CO, 1998, p. 599.

11. Conley, P. A., Benson, D. J., and Howe, P. M., "Microstructural Effects in Shock Initiation," Eleventh International Detonation Symposium, Office of Naval Research ONR 33300-5, Snowmass, CO, 1998, p. 768.

12. Tarver, C. M., Urtiew, P. A., Chidester, S. K., and Green, L. G., "Shock Compression and Initiation of LX-10," Propellants, Explosives, Pyrotechnics **18**, 117 (1993).

13. Fried, L., Howard, W. M., and Souers, P. C., "EXP6: A New Equation of State Library for High Pressure Thermochemistry," paper presented at this Symposium.

14. Maienschein, J. L. and Chandler, J. B., "Burn Rates of Pristine and Degraded Explosives at Elevated Temperatures and Pressures," Eleventh International Detonation Symposium, Office of Naval Research ONR 33300-5, Snowmass, CO, 1998, p. 872.

15. Farber, D. L., Zaug, J. M., and Ruddle, C., "First Results of Reaction Propagation Rates in HMX at High Pressures," Shock Compression of Condensed Matter-2001, Furnish, M. D., Thadhani, N. N., and Horie, Y, eds. CP-620, AIP Press, New York, 2002, in press.

16. Tarver, C. M., Cook, T. M., Urtiew, P. A., and Tao, W. C., "Multiple Shock Initiation of LX-17," Tenth International Detonation Symposium, Office of Naval Research ONR 33395-12, Boston, MA, 1993, p. 696.

17. Whitworth, N. J. and Maw, J. R., "Modeling Shock Desensitization of Heterogeneous Explosives," Shock Compression of Condensed Matter-1995, Schmidt, S. C. and Tao, W. C., eds., AIP Conference Proceedings 370, AIP Press, New York, 1996, p. 425.